Multimode Theory of Up-Conversion of Two Photons

Masatoshi Nakatani[1*], Ryosuke Shimizu[2,3], and Kazuki Koshino[1,2]

[1]*College of Liberal Arts and Sciences, Tokyo Medical and Dental University, Ichikawa, Chiba 272-0827*
[2]*PRESTO, Japan Science and Technology Agency, Kawaguchi, Saitama 332-0012*
[3]*Research Institute of Electrical Communication, Tohoku University, Sendai 980-8577*

The up-conversion dynamics of two photons in a three-level system is investigated theoretically. The analysis is based on a rigorous formalism that incorporates the multimode nature of the photon field, enabling quantitative handling of the spatial profiles of the photon pulses. We have derived an analytic formula that connects the wavefunction of two input photons to that of an up-converted output photon. The up-conversion efficiency and the output pulse profile are numerically calculated using this formula.

1. Introduction

In quantum information technologies, such as quantum cryptography and quantum computation,[1–3] nonlinear optical phenomena have many important applications, including generation of entangled photon pairs and construction of quantum gates. Up-conversion of two photons is a representative second-order nonlinear optical phenomenon, in which two incident photons are converted into a single photon with the sum frequency. In particular, this phenomenon can be utilized to realize a high-speed and long-distance quantum key distribution in telecommunication bands. Techniques for high-efficiency photon counting are rapidly improving by using up-conversion.[4–7]

The up-conversion dynamics of two photons can be qualitatively described by the phenomenological time evolution operator $\hat{U}$ based on the single-mode approximation $\hat{U} = \exp[-it\chi(b^\dagger aa + a^\dagger a^\dagger b)]$, where a and b are the annihilation operators for the input and up-converted photons, respectively, t is the interaction time, and χ is the coupling constant, which is proportional to the second-order nonlinear susceptibility.[8] However, optical nonlinear effects are sensitive to the spatial profiles of photon pulses, and the up-conversion efficiency can be affected by the pulse profiles of incident photons. This implies that the phenomenological approach based on the single-mode approximation is inadequate for quantitative engineering of photonic quantum states for novel quantum technologies. Therefore, a multimode analysis of the up-conversion dynamics that accounts for the spatial profiles of photons must be developed.

In this study, we develop a multimode theory of up-conversion dynamics of two photons. The analytical expression for the wavefunction of an up-converted photon is obtained as a function of the input wavefunction by using the method developed in refs. 9–11. A photon pulse has conventionally been characterized by its spatial profile, which is obtained from the first-order correlations of the photon field. However, the input state is not completely characterized by pulse profiles since it is possible to have input photons that have identical pulse profiles but different quantum states. We consider three types of photon pulses as input states. They have identical pulse profiles and are indistinguishable using classical measurements based on photon counting, where we define classical measurements as measurements of the first-order correlations of the photon field. It is demonstrated that these three input states induce different up-conversion dynamics.

This paper is organized as follows. In §2, we introduce a theoretical model for analyzing the up-conversion dynamics of two photons. As the simplest $\chi^{(2)}$-system, we consider a three-level system (referred to hereafter as "atom"). In §3, we present a formula that analytically connects the wavefunction of two input photons with the wavefunction of an up-converted photon. The obtained analytic result is described in §4, in which the up-conversion probability and the pulse profile of the up-converted photon are calculated numerically. Section 5 shows a summary of the study.

2. Theoretical Model

2.1 Hamiltonian

As illustrated in Fig. 1, the system considered in this study is composed of a one-dimensional photon field and a three-level atom located at $r = 0$. Such a situation can be realized experimentally by using a cavity quantum electrodynamics system in the weak-coupling regime.[12] Two photons are input from the input port (the $r < 0$ region) onto the atom, which is initially in the ground state. The atom has three energy levels, namely, $|g\rangle$, $|m\rangle$, and $|e\rangle$, as shown in Fig. 1. The energies $|e\rangle$ and $|m\rangle$ measured from $|g\rangle$ are denoted by Ω_e and Ω_m, respectively, and the decay rates associated with the $|e\rangle \to |g\rangle$, $|e\rangle \to |m\rangle$, and $|m\rangle \to |g\rangle$ transitions are denoted by Γ_1, Γ_2, and Γ_3, respectively. Employing natural units ($\hbar = c = 1$), the Hamiltonian for the overall system is given by

$$\mathcal{H} = \Omega_e \sigma_{ee} + \Omega_m \sigma_{mm} + \int dk\, k a_k^\dagger a_k$$
$$+ \int dk \left[i\sqrt{\frac{\Gamma_1}{2\pi}} \sigma_{eg} a_k + i\sqrt{\frac{\Gamma_2}{2\pi}} \sigma_{em} a_k \right.$$
$$\left. + i\sqrt{\frac{\Gamma_3}{2\pi}} \sigma_{mg} a_k + \text{H.c.} \right], \quad (1)$$

*Present address: Department of Physics and Electronics, Osaka Prefecture University, 1-1 Gakuen-cho, Naka-ku, Sakai 599-8531.

J. Phys. Soc. Jpn., Vol. 78, No. 5
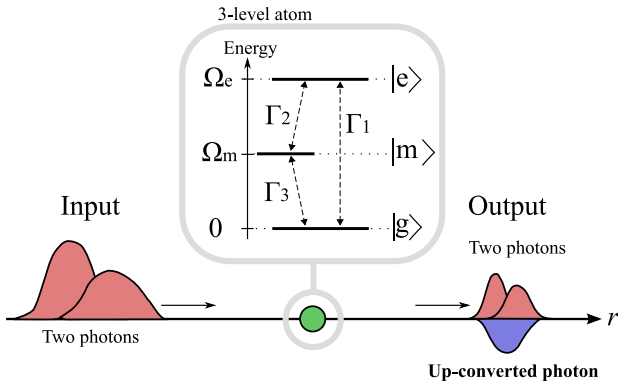
M. NAKATANI *et al.*

Fig. 1. (Color online) Physical situation investigated in this study. Two photons are input from the input port (the $r < 0$ region) onto a three-level atom located at $r = 0$. After interacting with the atom, an up-converted photon is generated in the output port (the $r > 0$ region) with a certain probability.

where a_k denotes the photon annihilation operator with the wave number k, and atomic transition operators are defined as $\sigma_{eg} = |e\rangle\langle g|$, for example. The real-space representation of the photon annihilation operator is defined as the Fourier transform of a_k so that

$$\tilde{a}_r = \frac{1}{\sqrt{2\pi}} \int dk \, a_k e^{ikr}. \tag{2}$$

2.2 Input two-photon states

The three types of two input photons that we consider in this study are depicted in Fig. 2. To characterize these states, we first introduce two *single-photon* modes, $\xi_1(r)$ and $\xi_2(r)$, which are shown in Fig. 2(a). [Specific forms of these functions are given later, see eqs. (17) and (18).] These mode functions are spatially separated and localized in the input port ($r < 0$ region). They are normalized as $\int dr |\xi_1(r)|^2 = \int dr |\xi_2(r)|^2 = 1$.

The two photons in Fig. 2(a) occupy different modes. This state is referred to as the spatially *anticorrelated* state. In contrast, the two photons in Fig. 2(b) occupy the same mode, ξ_1 or ξ_2, and the photonic state consists of their superpositions with equal weights. This state is referred to as the spatially *correlated* state.
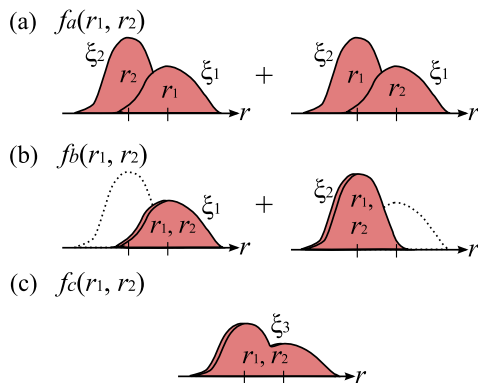

Fig. 2. (Color online) Schematic illustrations of the input two-photon states considered in this study: (a) spatially anticorrelated, (b) spatially correlated, and (c) spatially uncorrelated states. These three states have the same intensity distribution and are therefore indistinguishable by classical measurements.

In the multimode notation, the state vector of two-photon states can generally be cast in the following form:

$$|\psi_{in}^j\rangle = \iint dr_1 \, dr_2 \frac{f_j(r_1, r_2)}{\sqrt{2}} \tilde{a}_{r_1}^\dagger \tilde{a}_{r_2}^\dagger |0\rangle, \tag{3}$$

where $|0\rangle$ represents the overall ground state (the product of the atomic ground state and the photonic vacuum state), $f_j(r_1, r_2)$ is the two-photon wavefunction, and the index j ($= a, b, c$) discriminates the types of the two input photons. The wavefunctions for the anticorrelated ($j = a$) and correlated ($j = b$) photons are given by

$$f_a(r_1, r_2) = \frac{\xi_1(r_1)\xi_2(r_2) + \xi_2(r_1)\xi_1(r_2)}{\sqrt{2 + 2|\mathcal{V}|^2}}, \tag{4}$$

$$f_b(r_1, r_2) = \frac{\xi_1(r_1)\xi_1(r_2) + \xi_2(r_1)\xi_2(r_2)}{\sqrt{2 + 2\,\mathrm{Re}(\mathcal{V}^2)}}, \tag{5}$$

where $\mathcal{V}$ is the overlap between ξ_1 and ξ_2, defined by

$$\mathcal{V} = \int dr \, \xi_1(r)\xi_2^*(r). \tag{6}$$

These two-photon wavefunctions are normalized as $\int dr_1 \, dr_2 |f_j(r_1, r_2)|^2 = 1$ and symmetrized as $f_j(r_1, r_2) = f_j(r_2, r_1)$. The spatial profile of these two-photon pulses can be characterized by the intensity distribution function $I_{in}^j(r)$, which is defined by $I_{in}^j(r) = \langle \psi_{in}^j | \tilde{a}_r^\dagger \tilde{a}_r | \psi_{in}^j \rangle$ and normalized as $\int dr I_{in}^j(r) = n$ for n-photon states. From eqs. (4) and (5), we obtain

$$I_{in}^a(r) = \frac{|\xi_1(r)|^2 + |\xi_2(r)|^2 + [\mathcal{V}^*\xi_1(r)\xi_2^*(r) + \text{c.c.}]}{1 + |\mathcal{V}|^2}, \tag{7}$$

$$I_{in}^b(r) = \frac{|\xi_1(r)|^2 + |\xi_2(r)|^2 + [\mathcal{V}\xi_1(r)\xi_2^*(r) + \text{c.c.}]}{1 + \mathrm{Re}(\mathcal{V}^2)}. \tag{8}$$

In addition to the anticorrelated ($j = a$) and correlated ($j = b$) two-photon states, we define here the spatially *uncorrelated* ($j = c$) two-photon states, which have the same intensity profile as the anticorrelated state. For this purpose, we introduce a new single-photon mode function $\xi_3(r)$ satisfying $|\xi_3(r)|^2 = I_{in}^a(r)/2$, as shown in Fig. 2(c). The uncorrelated state is obtained by filling two photons in the mode $\xi_3(r)$. Therefore, the wavefunction f_c is given by

$$f_c(r_1, r_2) = \xi_3(r_1)\xi_3(r_2). \tag{9}$$

The state vector is given by eq. (3) with $j = c$. By definition, the pulse profile I_{in}^c for this state is identical to that for the anticorrelated state, namely,

$$I_{in}^c(r) = I_{in}^a(r). \tag{10}$$

In the following, we mainly consider the case in which $\mathcal{V}$ is real, which can be achieved by appropriate selection of the relative phase between ξ_1 and ξ_2. The pulse profiles of these three states (I_{in}^a, I_{in}^b, and I_{in}^c) become identical in this case. This indicates that these three input states are indistinguishable by classical measurements based on photon counting. However, it will be revealed in later sections that the nonlinear responses are sensitive to the type of input two-photon state.

3. Output Photons

The state vector of the output photons is determined by the Schrödinger equation

$$|\psi_{\text{out}}^j\rangle = e^{-i\mathcal{H}t}|\psi_{\text{in}}^j\rangle, \qquad (11)$$

where the final moment t is a sufficiently large time at which the atom is completely de-excited. The output state may include, with a certain probability, an up-converted photon associated with the $|e\rangle \rightarrow |g\rangle$ transition. The output state vector can thus be written as

$$|\psi_{\text{out}}^j\rangle = \iint dr_1\, dr_2\, \frac{g_j(r_1, r_2; t)}{\sqrt{2}} \tilde{a}_{r_1}^\dagger \tilde{a}_{r_2}^\dagger |0\rangle \\ + \int dr\, h_j(r; t)\tilde{a}_r^\dagger|0\rangle, \qquad (12)$$

where h_j and g_j are the one- and two-photon wavefunctions for the output, respectively. The up-conversion probability $P_j^{(1)}$ is given as the norm of h_j by

$$P_j^{(1)} = \int dr\, |h_j(r; t)|^2. \qquad (13)$$

Although this quantity depends on the final moment t by definition, it becomes independent of t for sufficiently large values. Similarly, the probability $P_j^{(2)}$ for the absence of up-conversion is given as the norm of g_j by

$$P_j^{(2)} = \iint dr_1\, dr_2\, |g_j(r_1, r_2; t)|^2 \qquad (14)$$

$$= 1 - P_j^{(1)}. \qquad (15)$$

As shown in Appendix, the Schrödinger equation (11) can be solved analytically. The wavefunction $h_j(r; t)$ of the up-converted photon is given in terms of the input wavefunction $f_j(r_1, r_2)$ by

$$h_j(r; t) = -\sqrt{2\Gamma_1 \Gamma_2 \Gamma_3}\, \exp\left[-\left(i\Omega_e + \frac{\Gamma_1 + \Gamma_2}{2}\right)(t - r)\right] \int_0^{t-r} d\tau_1 \int_0^{\tau_1} d\tau_2$$
$$\times \exp\left\{\left[i(\Omega_e - \Omega_m) + \frac{\Gamma_1 + \Gamma_2 - \Gamma_3}{2}\right]\tau_1\right\} \exp\left[\left(i\Omega_m + \frac{\Gamma_3}{2}\right)\tau_2\right] f_j(-\tau_1, -\tau_2). \qquad (16)$$

4. Numerical Results

In this section, we visualize the analytical result for eq. (16) and observe the differences in the up-conversion dynamics induced by the three different input states, namely, the anticorrelated state ($j = a$), the correlated state ($j = b$), and the uncorrelated state ($j = c$). For this purpose, we employ the following assumptions in this section: (i) Regarding the atomic energy, $\Omega_m = \Omega_e/2 \,(= \Omega)$. (ii) For the atomic decay rates, $\Gamma_1 = \Gamma_2 = \Gamma_3 \,(= \Gamma)$ and Γ^{-1} are used as the units of time and length, respectively. (iii) The two input photons are resonant to the $|g\rangle \rightarrow |m\rangle$ and $|m\rangle \rightarrow |e\rangle$ transitions. The input mode functions ξ_1 and ξ_2 are specified by eqs. (17) and (18), respectively.

4.1 Input mode functions

In this section, we assume the following forms for the input mode functions $\xi_1(r)$ and $\xi_2(r)$:

$$\xi_1(r) = \left(\frac{2}{\pi l^2}\right)^{1/4} \exp\left[-\left(\frac{r - a + d/2}{l}\right)^2 + i\Omega r\right], \qquad (17)$$

$$\xi_2(r) = \left(\frac{2}{\pi l^2}\right)^{1/4} \exp\left[-\left(\frac{r - a - d/2}{l}\right)^2 + i\Omega r\right], \qquad (18)$$

where l is the coherence length, d is the distance between $\xi_1(r)$ and $\xi_2(r)$, and $a(< 0)$ represents the initial position of the two photons. a is a redundant parameter provided that $|a| \gg l, d$, as is assumed here. The overlap $\mathcal{V}$ is given by $\mathcal{V} = \exp(-d^2/2l^2)$. The mode function $\xi_3(r)$ is defined by $\xi_3(r) = \sqrt{I_{\text{in}}^a(r)/2}\, \exp(i\Omega r)$. From eqs. (7), (17), and (18), we obtain

$$\xi_3(r) = \left(\frac{2}{\pi l^2}\right)^{1/4} \exp\left[-\left(\frac{r - a}{l}\right)^2 + i\Omega r\right] \\ \times \left\{\frac{\cosh[2(r - a)d/l^2] + e^{-d^2/2l^2}}{2\cosh(d^2/2l^2)}\right\}^{1/2}. \qquad (19)$$

The profiles of these mode functions ($|\xi_1|$, $|\xi_2|$, and $|\xi_3|$) are shown in Fig. 3. The two-photon wavefunctions (f_a, f_b, and
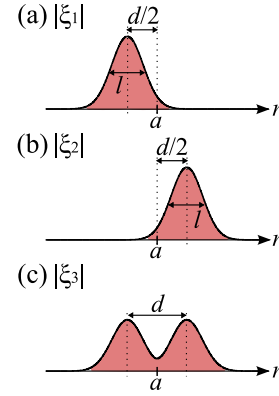

Fig. 3. (Color online) Profiles of the input mode functions assumed in this study. The mode functions ξ_1 and ξ_2 have peaks at $r = a - d/2$ and $r = a + d/2$, respectively. The coherence length l is the width of the peaks. The mode function ξ_3 has two peaks at $r = a - d/2$ and $r = a + d/2$. The mode distance d is the distance between these two peaks for this mode.

f_c) are given by eqs. (4), (5), and (9), respectively. It should be stressed that the overlap $\mathcal{V}$ is real in the present case, and that the pulse profiles (I_{in}^a, I_{in}^b, and I_{in}^c) become completely identical. Therefore, these three input states are indistinguishable by classical measurements.

4.2 Up-conversion probability

From the two-photon wavefunctions f_j ($j = a, b, c$), the wavefunction h_j of the up-converted photon can be obtained numerically by using eq. (16). In this subsection, we discuss the up-conversion probability $P_j^{(1)}$, which is given by eq. (13), as the norm of h_j.

First, we examine the dependence of the up-conversion efficiency $P_j^{(1)}$ on the coherence length l by fixing the distance d at 0. The up-conversion probability is plotted in Fig. 4 as a function of l. Note that the three input states (f_a, f_b, and f_c) become identical in the present case of $d = 0$. Figure 4 shows that there exists an optimum coherence
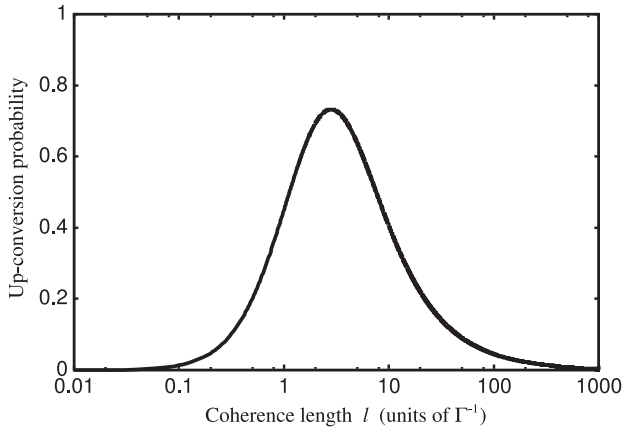
Fig. 4. Up-conversion probability as a function of the coherence length l. The mode distance is fixed at $d = 0$, where the three types of input states become identical. The up-conversion efficiency is optimized when $l \simeq 3\Gamma^{-1}$.
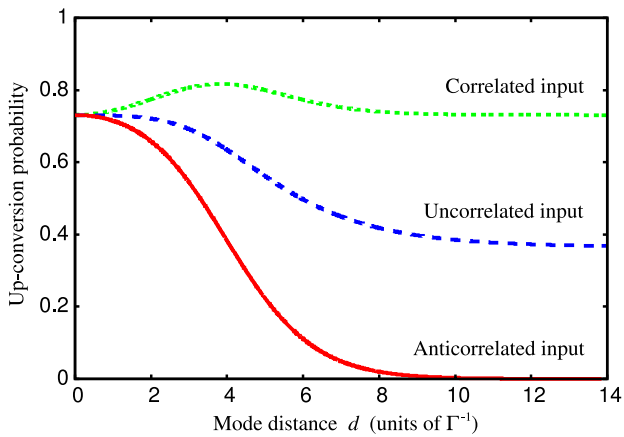

Fig. 5. (Color online) Up-conversion probabilities as functions of the mode distance d. The coherence length is fixed at $l = 3\Gamma^{-1}$. The solid, dotted, and dashed lines show the results for the anticorrelated, correlated, and uncorrelated inputs, respectively.

length for inducing up-conversion. In the $l \to 0$ limit, the input photons become spectrally broad and cannot interact with the atom effectively. On the other hand, in the $l \to \infty$ limit, the field strength of the photons decreases such that it cannot induce the $|g\rangle \to |m\rangle$ transition efficiently. The up-conversion probability is maximized when $l \simeq 3\Gamma^{-1}$, as shown in Fig. 4.

Next, we examine the dependence of $P_j^{(1)}$ on the mode distance d by fixing the coherence length l at $3\Gamma^{-1}$. The up-conversion probabilities for the three input states ($|\Psi_{\mathrm{in}}^a\rangle$, $|\Psi_{\mathrm{in}}^b\rangle$, and $|\Psi_{\mathrm{in}}^c\rangle$) are plotted in Fig. 5 as functions of d. When $d = 0$, the three probabilities coincide, as depicted in Fig. 5, because the three input states become identical in this case. In contrast, differences become apparent as the mode distance d increases: The up-conversion probability $P_a^{(1)}$ vanishes in the $d \to \infty$ limit for the anticorrelated input (solid line in Fig. 5), whereas $P_b^{(1)}$ remains almost unchanged even in the $d \to \infty$ limit for the correlated input (dotted line in Fig. 5). This can be qualitatively understood by the fact that the arrival of two photons at the atom within a short time interval is essential for up-conversion, because the first

excitation ($|g\rangle \to |m\rangle$) should be followed immediately by the second excitation ($|m\rangle \to |e\rangle$) before the relaxation ($|m\rangle \to |g\rangle$). As Fig. 2 shows, when the mode distance d is increased, the distance between the two photons necessarily increases for the anticorrelated input, whereas the two photons always arrive at the atom within a short time interval for the correlated input.

It is observed that there is a maximum point at $d \simeq 4\Gamma^{-1}$ for the correlated input in Fig. 5. This arises from the quantum interference between $\xi_1(r_1)\xi_1(r_2)$ and $\xi_2(r_1)\xi_2(r_2)$. In contrast, such quantum interference does not occur for the anticorrelated input since $\xi_1(r_1)\xi_2(r_2) = \xi_2(r_1)\xi_1(r_2)$ from eqs. (17) and (18).

The uncorrelated input (dashed line in Fig. 5) yields intermediate results between the correlated and anticorrelated inputs. This is because the uncorrelated input can be regarded as a superposition of the correlated and anticorrelated inputs. In particular, in the $d \to \infty$ limit, $\xi_3 \simeq (\xi_1 + \xi_2)/\sqrt{2}$ from eq. (19), and $f_c \simeq (f_a + f_b)/\sqrt{2}$ from eq. (9). Therefore, $P_c^{(1)}$ is approximately given by $P_c^{(1)} \simeq (P_a^{(1)} + P_b^{(1)})/2$, as can be confirmed in Fig. 5.

4.3 Pulse profile of up-converted photon

Another physical quantity extractable from h_j is the pulse profile $I_j^{(1)}(r)$ of the up-converted photon, which is defined by

$$I_j^{(1)}(r) = |h_j(r;t)|^2. \tag{20}$$

The norm of the pulse profile gives the up-conversion probability as $\int dr\, I_j^{(1)}(r) = P_j^{(1)}$.

The pulse profiles $I_j^{(1)}(r)$ of the up-converted photon are plotted in Fig. 6. Figure 6(a) shows the results for the case when the mode functions $\xi_1(r)$ and $\xi_2(r)$ are well separated ($d \gg l$). For the anticorrelated input [solid line in Fig. 6(a)], the up-converted photon is generated in the region in which $\xi_1(r)$ and $\xi_2(r)$ overlap. On the other hand, for the correlated input [dotted line in Fig. 6(a)], the up-converted photon is generated at the positions of $\xi_1(r)$ and $\xi_2(r)$ with almost identical weights. This can be understood by the fact that an up-converted photon can be generated if two input photons arrive at the atom within a short time interval. For the uncorrelated input [dashed line in Fig. 6(a)], the intensity $I_c^{(1)}(r)$ is nearly one-half of $I_b^{(1)}(r)$. This is because the uncorrelated input is given by $f_c \simeq (f_a + f_b)/\sqrt{2}$ when $\xi_1(r)$ and $\xi_2(r)$ are well separated, and the anticorrelated input f_a makes a negligible contribution. As the two modes $\xi_1(r)$ and $\xi_2(r)$ become closer ($d \sim l$), the discrimination between the three inputs gradually disappears. The profile of the up-converted photon assumes a complex asymmetric form due to quantum interference [see Fig. 6(b)].

It is thus demonstrated that, although the three input states have identical pulse profiles and are therefore indistinguishable by classical measurements, the up-conversion dynamics induced by them are different. As shown in Fig. 5, a high up-conversion efficiency is obtained when a correlated two-photon pulse is input. Therefore, the correlated two-photon pulse is advantageous for maximizing the nonlinear optical effects.

5. Summary

The up-conversion dynamics of two photons is inves-

J. Phys. Soc. Jpn., Vol. 78, No. 5
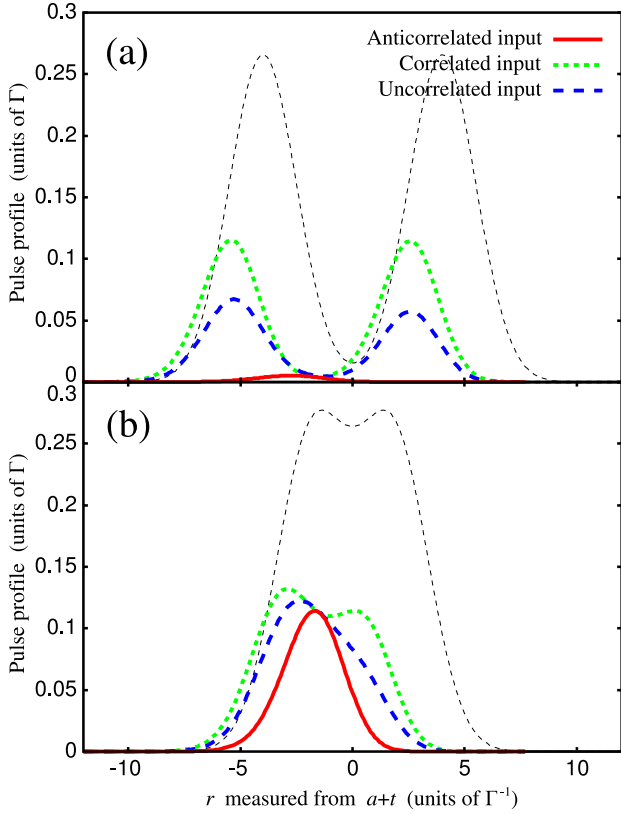
M. NAKATANI *et al.*

Fig. 6. (Color online) Pulse profiles of the up-converted photon. Results for the anticorrelated, correlated, and uncorrelated inputs are indicated by the solid, dotted, and dashed lines, respectively. In (a), the parameters are set at $l = 3\Gamma^{-1}$ and $d = 8\Gamma^{-1}$ (the $d \gg l$ case), whereas in (b), they are set at $l = 3\Gamma^{-1}$ and $d = 4\Gamma^{-1}$ (the $d \sim l$ case). The input pulse profiles (which are identical for the three kinds of inputs) are indicated by a thin dashed line.

tigated theoretically, assuming a three-level system as the simplest second-order nonlinear optical system. The analysis is based on a rigorous formalism in which both photons and optical media are treated quantum-mechanically and the multimode nature of the photon field is considered. Three types of states are considered for the input two-photon state: spatially *anticorrelated*, *correlated*, and *uncorrelated* states, which are schematically illustrated in Fig. 2. These three states have an identical pulse profile and are therefore indistinguishable by classical measurements.

We have derived eq. (16), which connects the two-photon wavefunction $f_j(r_1, r_2)$ in the input port with the one-photon wavefunction $h_j(r, t)$ of the up-converted photon in the output port. From $h_j(r, t)$, we have evaluated the up-conversion probability [eq. (13) and Fig. 5] and the pulse profile [eq. (20) and Fig. 6]. It is found that, although the three input states are indistinguishable on the basis of their intensity distributions, they induce different up-conversion dynamics. These results demonstrate the necessity of using multimode treatment for photons in quantitative theories of nonlinear quantum optics.

Appendix: Derivation of Wavefunction of Up-Converted Photon

In this appendix, the wavefunction of the up-converted photon is analytically derived. The wavefunction is expressed as a function of the input two-photon wavefunction $f_j(r_1, r_2)$, as shown in eq. (16). In order to calculate the wavefunction of the up-converted photon, we use the method developed in refs. 9–11.

A.1 Coherent input and corresponding output states
A.1.1 Coherent input state

We consider the following coherent state as the input:

$$|\phi_{\text{in}}\rangle = \mathcal{N} \exp\left\{\int dr[\mu\xi_1(r) + \nu\xi_2(r)]\tilde{a}_r^\dagger\right\}|0\rangle, \qquad \text{(A·1)}$$

where $\mathcal{N} = \exp[-(|\mu|^2 + |\nu|^2 + \mu\nu^*\mathcal{V} + \mu^*\nu\mathcal{V}^*)/2]$ and μ and ν are perturbation parameters. This state has the photon amplitude $\mathcal{F}(r; 0) = \langle\phi_{\text{in}}|\tilde{a}_r|\phi_{\text{in}}\rangle = \mu\xi_1(r) + \nu\xi_2(r)$. Expanding in powers of μ and ν, the state $|\phi_{\text{in}}\rangle$ is written as

$$|\phi_{\text{in}}\rangle = |0\rangle + \mu|\xi_1\rangle + \nu|\xi_2\rangle + \frac{\mu^2}{\sqrt{2}}|\xi_1\xi_1\rangle + \frac{\nu^2}{\sqrt{2}}|\xi_2\xi_2\rangle$$
$$+ \mu\nu\sqrt{1 + |\mathcal{V}|^2}|\xi_1\xi_2\rangle + \cdots, \qquad \text{(A·2)}$$

where the state vectors on the right-hand side are given by, for example,

$$|\xi_1\rangle = \int dr\, \xi_1(r)\tilde{a}_r^\dagger|0\rangle, \qquad \text{(A·3)}$$

$$|\xi_1\xi_1\rangle = \iint dr_1\, dr_2 \frac{\xi_1(r_1)\xi_1(r_2)}{\sqrt{2}} \tilde{a}_{r_1}^\dagger \tilde{a}_{r_2}^\dagger|0\rangle, \qquad \text{(A·4)}$$

$$|\xi_1\xi_2\rangle = \iint dr_1\, dr_2 \frac{\xi_1(r_1)\xi_2(r_2)}{\sqrt{1 + |\mathcal{V}|^2}} \tilde{a}_{r_1}^\dagger \tilde{a}_{r_2}^\dagger|0\rangle. \qquad \text{(A·5)}$$

Note that in terms of these states, the anticorrelated and correlated states can be written as $|\psi_{\text{in}}^a\rangle = |\xi_1\xi_2\rangle$ and $|\psi_{\text{in}}^b\rangle = (|\xi_1\xi_1\rangle + |\xi_2\xi_2\rangle)/\sqrt{2 + 2\operatorname{Re}(\mathcal{V}^2)}$, respectively.

A.1.2 Corresponding output state

From the linearity of the Schrödinger equation $|\phi_{\text{out}}\rangle = e^{-i\mathcal{H}t}|\phi_{\text{in}}\rangle$, the output state for this coherent input state can be given by

$$|\phi_{\text{out}}\rangle = |0\rangle + \mu|\xi_{1\text{out}}\rangle + \nu|\xi_{2\text{out}}\rangle + \frac{\mu^2}{\sqrt{2}}|\xi_1\xi_{1\text{out}}\rangle$$
$$+ \frac{\nu^2}{\sqrt{2}}|\xi_2\xi_{2\text{out}}\rangle + \frac{\mu\nu}{\sqrt{2}}|\xi_1\xi_{2\text{out}}\rangle + \cdots, \qquad \text{(A·6)}$$

where we write the state vectors on the right-hand side in the following forms:

$$|\xi_{1\text{out}}\rangle = \int dr\, \zeta_1(r; t)\tilde{a}_r^\dagger|0\rangle, \qquad \text{(A·7)}$$

$$|\xi_1\xi_{1\text{out}}\rangle = \iint dr_1\, dr_2 \frac{\zeta_{11}(r_1, r_2; t)}{\sqrt{2}} \tilde{a}_{r_1}^\dagger \tilde{a}_{r_2}^\dagger|0\rangle$$
$$+ \int dr\, \eta_{11}(r; t)\tilde{a}_r^\dagger|0\rangle, \qquad \text{(A·8)}$$

$$|\xi_1\xi_{2\text{out}}\rangle = \iint dr_1\, dr_2 \frac{\zeta_{12}(r_1, r_2; t)}{\sqrt{2}} \tilde{a}_{r_1}^\dagger \tilde{a}_{r_2}^\dagger|0\rangle$$
$$+ \int dr\, \eta_{12}(r; t)\tilde{a}_r^\dagger|0\rangle. \qquad \text{(A·9)}$$

The wavefunctions of the output two-photon states are denoted by $\zeta_{11}(r_1, r_2; t)$ and $\zeta_{12}(r_1, r_2; t)$, and $\zeta_1(r; t)$ is the wavefunction of the output one-photon state with the fundamental frequency, whereas, $\eta_{11}(r; t)$ and $\eta_{12}(r; t)$ denote the wavefunctions of the output one-photon states

with the sum frequency, which are the up-converted photon states. We write the state vectors $|\xi_{2\text{out}}\rangle$ and $|\xi_2\xi_{2\text{out}}\rangle$ in a similar manner. Considering that we can write $|\psi_{\text{out}}^a\rangle = |\xi_1\xi_{2\text{out}}\rangle$ and $|\psi_{\text{out}}^b\rangle = (|\xi_1\xi_{1\text{out}}\rangle + |\xi_2\xi_{2\text{out}}\rangle)/\sqrt{2 + 2\,\text{Re}(\mathcal{V}^2)}$, the following relations can be obtained:

$$h_a(r;t) = \eta_{12}(r;t), \tag{A.10}$$

$$h_b(r;t) = \frac{\eta_{11}(r;t) + \eta_{22}(r;t)}{\sqrt{2 + 2\,\text{Re}(\mathcal{V}^2)}}. \tag{A.11}$$

A.2 Input–output relation and field amplitude

From the Heisenberg equation for the field operator a_k, we obtain the following input–output relation

$$\tilde{a}_r(t) = \tilde{a}_{r-t}(0) - \sqrt{\Gamma_1}\sigma_{\text{ge}}(t-r) - \sqrt{\Gamma_2}\sigma_{\text{me}}(t-r) \\ - \sqrt{\Gamma_3}\sigma_{\text{gm}}(t-r). \tag{A.12}$$

Using this input–output relation, the photon amplitude of the corresponding output state, which is given by $\mathcal{F}(r;t) = \langle\phi_{\text{out}}|\tilde{a}_r|\phi_{\text{out}}\rangle = \langle\phi_{\text{in}}|\tilde{a}_r(t)|\phi_{\text{in}}\rangle \equiv \langle\tilde{a}_r(t)\rangle$, can be expressed in two ways as

$$\mathcal{F}(r;t) = \mu\zeta_1(r;t) + \nu\zeta_2(r;t) + \frac{\mu^2}{\sqrt{2}}\eta_{11}(r;t) + \frac{\nu^2}{\sqrt{2}}\eta_{22}(r;t) \\ + \mu\nu\sqrt{1 + |\mathcal{V}|^2}\,\eta_{12}(r;t) + \cdots, \tag{A.13}$$

$$= \mu\xi_1(r-t) + \nu\xi_2(r-t) - \sqrt{\Gamma_1}\langle\sigma_{\text{ge}}(t-r)\rangle \\ - \sqrt{\Gamma_2}\langle\sigma_{\text{me}}(t-r)\rangle - \sqrt{\Gamma_3}\langle\sigma_{\text{gm}}(t-r)\rangle. \tag{A.14}$$

Therefore, comparing the components of the same order for μ and ν, the following relations can be obtained:

$$\eta_{11}(r;t) = -\sqrt{2\Gamma_1}\langle\sigma_{\text{ge}}(t-r)\rangle^{(\mu^2)}, \tag{A.15}$$

$$\eta_{22}(r;t) = -\sqrt{2\Gamma_1}\langle\sigma_{\text{ge}}(t-r)\rangle^{(\nu^2)}, \tag{A.16}$$

$$\eta_{12}(r;t) = -\sqrt{\frac{\Gamma_1}{1 + |\mathcal{V}|^2}}\langle\sigma_{\text{ge}}(t-r)\rangle^{(\mu\nu)}, \tag{A.17}$$

where $\langle\sigma_{\text{ge}}(t-r)\rangle^{(\mu^2)}$ is the second-order component of $\langle\sigma_{\text{ge}}(t-r)\rangle = \langle\phi_{\text{in}}|\sigma_{\text{eg}}(t-r)|\phi_{\text{in}}\rangle$ proportional to μ^2, for example. From eqs. (A.10), (A.11), and (A.15)–(A.17), we can obtain

$$h_a(r;t) = -\sqrt{\frac{\Gamma_1}{1 + |\mathcal{V}|^2}}\langle\sigma_{\text{ge}}(t-r)\rangle^{(\mu\nu)}, \tag{A.18}$$

$$h_b(r;t) = -\sqrt{\frac{\Gamma_1}{1 + \text{Re}(\mathcal{V}^2)}} \\ \times [\langle\sigma_{\text{ge}}(t-r)\rangle^{(\mu^2)} + \langle\sigma_{\text{ge}}(t-r)\rangle^{(\nu^2)}]. \tag{A.19}$$

A.3 Equations of motion for atomic operators

The second-order components of the expectation $\langle\sigma_{\text{ge}}(t-r)\rangle$ in eqs. (A.18) and (A.19) can be calculated from the Heisenberg equations for the atomic operators σ_{gm} and σ_{ge}. From the Heisenberg equations for σ_{gm} and σ_{ge}, the equations of motion for $\langle\sigma_{\text{gm}}\rangle$ and $\langle\sigma_{\text{ge}}\rangle$ are given by

$$\frac{\text{d}}{\text{d}\tau}\langle\sigma_{\text{gm}}\rangle = -\left(i\Omega_{\text{m}} + \frac{\Gamma_3}{2}\right)\langle\sigma_{\text{gm}}\rangle - \frac{\sqrt{\Gamma_1\Gamma_3}}{2}\langle\sigma_{\text{ge}}\rangle \\ + \sqrt{\Gamma_1\Gamma_2}\langle\sigma_{\text{ee}}\rangle + \sqrt{\Gamma_2\Gamma_3}\langle\sigma_{\text{me}}\rangle \\ - \sqrt{\Gamma_1}[\mu\xi_1(-\tau) + \nu\xi_2(-\tau)]\langle\sigma_{\text{em}}\rangle$$

$$- \sqrt{\Gamma_2}[\mu^*\xi_1^*(-\tau) + \nu^*\xi_2^*(-\tau)]\langle\sigma_{\text{ge}}\rangle \\ - \sqrt{\Gamma_3}[\mu\xi_1(-\tau) + \nu\xi_2(-\tau)](\langle\sigma_{\text{mm}}\rangle - \langle\sigma_{\text{gg}}\rangle), \tag{A.20}$$

$$\frac{\text{d}}{\text{d}\tau}\langle\sigma_{\text{ge}}\rangle = -\left(i\Omega_{\text{e}} + \frac{\Gamma_1 + \Gamma_2}{2}\right)\langle\sigma_{\text{ge}}\rangle - \frac{\sqrt{\Gamma_1\Gamma_3}}{2}\langle\sigma_{\text{gm}}\rangle \\ - \sqrt{\Gamma_1}[\mu\xi_1(-\tau) + \nu\xi_2(-\tau)](\langle\sigma_{\text{ee}}\rangle - \langle\sigma_{\text{gg}}\rangle) \\ + \sqrt{\Gamma_2}[\mu\xi_1(-\tau) + \nu\xi_2(-\tau)]\langle\sigma_{\text{gm}}\rangle \\ - \sqrt{\Gamma_3}[\mu\xi_1(-\tau) + \nu\xi_2(-\tau)]\langle\sigma_{\text{me}}\rangle, \tag{A.21}$$

where we used the virtue of the coherent state: $\tilde{a}_r|\phi_{\text{in}}\rangle = [\mu\xi_1(r) + \nu\xi_2(r)]|\phi_{\text{in}}\rangle$. Using the rotating wave approximation, and expanding these equations in powers of μ and ν, it is found that, except for $\langle\sigma_{\text{ge}}\rangle$ and $\langle\sigma_{\text{gm}}\rangle$, the expectations of the atomic operators make no contribution to the equations of motion for the second-order components of $\langle\sigma_{\text{ge}}\rangle$, and that the second-order components of $\langle\sigma_{\text{me}}\rangle$ vanish for the initial condition $\langle\sigma_{\text{me}}(0)\rangle = 0$. Therefore, we can obtain the equations of motion for the second-order components of $\langle\sigma_{\text{ge}}\rangle$ as

$$\frac{\text{d}}{\text{d}\tau}\langle\sigma_{\text{ge}}\rangle^{(\mu^2)} = -\left(i\Omega_{\text{e}} + \frac{\Gamma_1 + \Gamma_2}{2}\right)\langle\sigma_{\text{ge}}\rangle^{(\mu^2)} \\ + \sqrt{\Gamma_2}\xi_1(-\tau)\langle\sigma_{\text{gm}}\rangle^{(\mu)}, \tag{A.22}$$

$$\frac{\text{d}}{\text{d}\tau}\langle\sigma_{\text{ge}}\rangle^{(\nu^2)} = -\left(i\Omega_{\text{e}} + \frac{\Gamma_1 + \Gamma_2}{2}\right)\langle\sigma_{\text{ge}}\rangle^{(\nu^2)} \\ + \sqrt{\Gamma_2}\xi_2(-\tau)\langle\sigma_{\text{gm}}\rangle^{(\nu)}, \tag{A.23}$$

$$\frac{\text{d}}{\text{d}\tau}\langle\sigma_{\text{ge}}\rangle^{(\mu\nu)} = -\left(i\Omega_{\text{e}} + \frac{\Gamma_1 + \Gamma_2}{2}\right)\langle\sigma_{\text{ge}}\rangle^{(\mu\nu)} \\ + \sqrt{\Gamma_2}[\xi_1(-\tau)\langle\sigma_{\text{gm}}\rangle^{(\nu)} + \xi_2(-\tau)\langle\sigma_{\text{gm}}\rangle^{(\mu)}]. \tag{A.24}$$

These equations involve the linear components of $\langle\sigma_{\text{gm}}\rangle$. We can obtain the equations of motion for the linear components of $\langle\sigma_{\text{gm}}\rangle$ from eq. (A.20) as

$$\frac{\text{d}}{\text{d}\tau}\langle\sigma_{\text{gm}}\rangle^{(\mu)} = -\left(i\Omega_{\text{m}} + \frac{\Gamma_3}{2}\right)\langle\sigma_{\text{gm}}\rangle^{(\mu)} \\ + \sqrt{\Gamma_3}\xi_1(-\tau), \tag{A.25}$$

$$\frac{\text{d}}{\text{d}\tau}\langle\sigma_{\text{gm}}\rangle^{(\nu)} = -\left(i\Omega_{\text{m}} + \frac{\Gamma_3}{2}\right)\langle\sigma_{\text{gm}}\rangle^{(\nu)} \\ + \sqrt{\Gamma_3}\xi_2(-\tau). \tag{A.26}$$

Solving these equations, the wavefunctions of the up-converted photon $h_j(r;t)$ can be obtained analytically as eq. (16). This expression for the wavefunctions of the up-converted photon is also derived for the uncorrelated photons f_c when we consider the coherent state $|\phi_{\text{in}}^c\rangle$ with the photon amplitude $\mathcal{F}_c(r;0) = \langle\phi_{\text{in}}^c|\tilde{a}_r|\phi_{\text{in}}^c\rangle = \lambda\xi_3(r)$ as input, where λ is a perturbation parameter. Therefore, given the input two-photon wavefunction $f_j(r_1, r_2)$, we can determine the specific expressions for $h_j(r;t)$ from eq. (16).

1) M. A. Nielsen and I. L. Chuang: *Quantum Computation and Quantum Information* (Cambridge University Press, Cambridge, U.K., 2000).
2) N. Gisin, G. Ribordy, W. Tittel, and H. Zbinden: Rev. Mod. Phys. **74** (2002) 145.

3) N. Gisin and R. Thew: Nat. Photonics **1** (2007) 165.
4) A. P. VanDevender and P. G. Kwiat: J. Mod. Opt. **51** (2004) 1433.
5) H. Takesue, E. Diamanti, T. Honjo, C. Langrock, M. M. Fejer, K. Inoue, and Y. Yamamoto: New J. Phys. **7** (2005) 232.
6) R. T. Thew, S. Tanzilli, L. Krainer, S. C. Zeller, A. Rochas, I. Rech, S. Cova, H. Zbinden, and N. Gisin: New J. Phys. **8** (2006) 32.
7) H. Takesue, S. W. Nam, Q. Zhang, R. H. Hadfield, T. Honjo, K.

Tamaki, and Y. Yamamoto: Nat. Photonics **1** (2007) 343.
8) F. Dell'Anno, S. D. Siena, and F. Illuminati: Phys. Rep. **428** (2006) 53.
9) K. Koshino and H. Ishihara: Phys. Rev. Lett. **93** (2004) 173601.
10) K. Koshino and H. Ishihara: Int. J. Mod. Phys. B **20** (2006) 2451.
11) K. Koshino: Phys. Rev. Lett. **98** (2007) 223902.
12) Q. A. Turchette, C. J. Hood, W. Lange, H. Mabuchi, and H. J. Kimble: Phys. Rev. Lett. **75** (1995) 4710.